Proceedings of Ninth World Conference on Earthquake Engineering
August 2-9, 1988, Tokyo-Kyoto, JAPAN (Vol.VI)

10-4-1

ESTIMATION OF SLOSHING WAVE HEIGHT IN VICINITY OF SOURCE REGION

Takashi OKAMOTO[1], Yoshikazu YAMADA[2] and Shigeru NODA[3]

[1]Civil & Building Technology Research Dept., Steel Research Center, NKK Corporation, Kawasaki-shi, Kanagawa, Japan
[2]Department of Civil Engineering, Faculty of Engineering, Kyoto University, Sakyo-ku, Kyoto, Japan
[3]Department of Social Systems Engineering, Faculty of Engineering, Tottori University, Tottori-shi, Tottori, Japan

SUMMARY

This paper presents the response analyses of the sloshing wave of tanks in the vicinity of a source region using the theoretical earthquake motion. The earthquake motion is calculated by applying the Discrete Wavenumber/Finite Element (DWFE) method proposed by Olson et al.(1982) and the fault dislocation theory. A hypothetical South-Kanto earthquake which corresponds to the Great Kanto earthquake of 1923 is assumed to have struck again. Sloshing waves of five kinds of tanks with capacities ranging from 40,000kl to 100,000kl are analyzed applying the axisymmetric linear potential theory. The wave heights of 2.3m-6.2m in Tokyo, and 3.4m-9.4m in Chiba prefecture are predicted.

INTRODUCTION

The clarification of sloshing behaviors plays an important role in design of liquid storage tanks. By the Nihonkai-chubu earthquake of 1983 (Middle-Japan Sea earthquake M=7.7), large sloshing wave heights in petroleum storage tanks were caused in Niigata city, and petroleum overflowed in some of them. With this as a turning point, the clarification of sloshing behaviors becomes widely recognized as important.

For the clarification of sloshing behaviors, it is necessary to examine a relatively long-period component of the earthquake records obtained in the vicinity of a source region of large earthquakes. However, there are not many earthquake records. In earthquake-proof design of storage tanks recommended by the Ministry of International Trade and Industry of Japan, a theoretical earthquake motion calculated by the fault model is used in sloshing analysis, in addition to actual earthquake records.

In this paper, assuming the recurrence of the Great Kanto earthquake(M=7.9) of 1923, a theoretical earthquake motion in the vicinity of a source region is calculated which includes a relatively long-period (2.5-20 sec) component. Using the theoretical earthquake motion, the sloshing behaviors are analyzed in large-scale storage tanks.

CALCULATION OF EARTHQUAKE MOTIONS BY THE DWFE METHOD

In the calculation of the theoretical earthquake motions, the Green function of a homogeneous layered medium is calculated by applying the Discrete

Wavenumber/ Finite Element method (DWFE method) proposed by Olson et al.(Ref. 1). In this method, wave equations are expanded in the Fourier-Bessel series in a horizontal direction, discretized by the finite element method in vertical direction, discretized by the finite difference method with respect to time, and solved numerically. The wave motions containing both body waves (P and S waves) and surface waves (Love and Rayleigh waves) can be calculated simultaneously. Therefore, the DWFE method is suitable for calculation of the earthquake motion in the vicinity of a source region. Furthermore, it gives less calculation time than the generalized ray method and the wavenumber integration method, etc.

GROUND MOTIONS FROM THE HYPOTHETICAL SOUTH-KANTO EARTHQUAKE

Fault model and model of crustal structure In this paper, the macro fault model of the Great Kanto earthquake proposed by Matsu'ura et al.(Ref. 2) is used. The fault model is deduced on the basis of the geodetic data by the inversion method. Parameters of this model are shown in Table 1. The position of the fault plane is shown in Fig. 1. The epicenter is located at (35.41°N,139.22°E) in Fig. 1 whose depth is 13.5km. As the model of crustal structure, the structure beneath Yumenoshima island near Tokyo obtained by Shima et al.(Ref. 3) is used. A homogeneous layered medium is assumed from the epicenter region to the observation site. The parameters of the model are shown in Table 2.

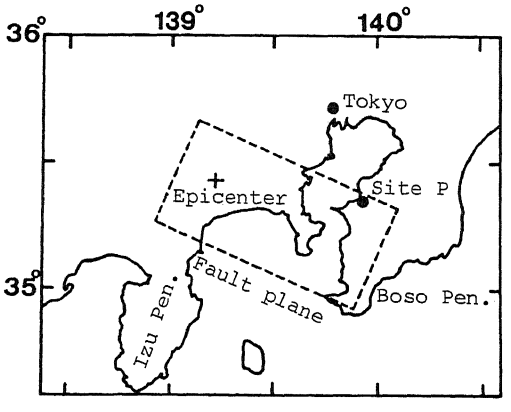

Fig. 1 Fault plane of hypothetical South-Kanto earthquake

Table 1 Macro fault parameters

Dislocation	D_0	4.8 m
Dip-Angle	δ	25° NE
Slip-Angle	λ	140°
Fault Width	W	54 km
Fault Length	L	95 km
Depth to upper fault margin	d	1.9 km
Strike direction	ϕ	N66° W
Seismic Moment	M_0	8.4×10^{27}dyne·cm
Rupture Velocity	V_R	2 km/sec
Rise Time	τ	5 sec

Table 2 Model of crustal structure

Depth (km)	Unit Weight (t/m^3)	Velocity of S-Wave (m/sec)	Velocity of P-Wave (m/sec)
0 ~ 1.3	2.0	680	1800
1.3~ 2.3	2.3	1500	2700
2.3~ 6.0	2.7	3000	5500
Over 6.0	2.8	3400	6200

DWFE method As shown in Fig. 2, the fault plane is subdivided into many small segments(10x5). The rupture in each segment is represented by four point sources which are placed on the corners of the segment. The point source (4,3) in Fig. 2 is the starting point of rupture. The rupture front propagates two-dimensionally with uniform velocity(V_R) from the epicenter on the fault. The number of rectangular segments on the fault is determined by the following factors(Ref. 4); distance between the fault plane and observation site, propagation velocity of earthquake motion, frequency range, calculation time and capacity of a computer. The distribution of seismic moment on the fault is assumed triangular in the direction of the fault width(Y-direction) and uniform in the direction of the fault length(X-direction) as shown in Fig. 3. For each point source, the uniform rise time and rupture velocity are assigned. Velocity function of dislocation, $A_0\dot{f}(t)$ ($A_0=3/2\tau D_0$), is adopted as shown in Fig. 4. In the DWFE method, the Green function in each point source is calculated for the period range from 2.5 to 20 sec. The value of time step Δt is taken as 0.15 sec. Calculated duration time of

earthquake motion is about 300 sec. In calculation of the Green function, the stability condition is determined by the following factors(Ref. 5); the frequency range and duration time of earthquake motion, the length of segment, and the velocity of P and S waves in each layer of crustal structure. The elemental waves due to every point source and the synthetic wave are corrected by the equi-ripple Chebyshev band pass filter, and the component of the period longer than 20 sec is removed.

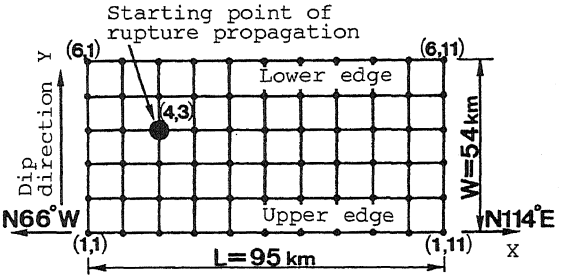

Fig. 2 Point sources on the fault plane

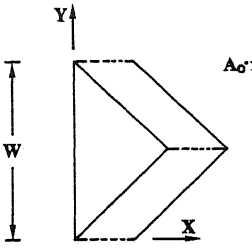

Fig. 3 Distribution of seismic moment

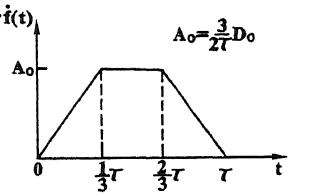

Fig. 4 Velocity function of dislocation

Earthquake motion at Hongo in Tokyo

In order to examine the validity of the present method, calculated earthquake motion in Tokyo is compared with the actual earthquake motion which was observed at Hongo in Tokyo during the Great Kanto earthquake of 1923. The calculated earthquake motion(SW-NE component) in Tokyo is shown in Fig. 5. Fig. 6 is the actual earthquake motion reproduced by Morioka(Ref. 6) from the incomplete record of an Ewing-type seismograph. The calculated motion does not contain the components of the period less than 2.5 sec, so that the agreement is not so good in the acceleration wave. However, good agreement is found for the maximum value of the displacement and velocity waves.

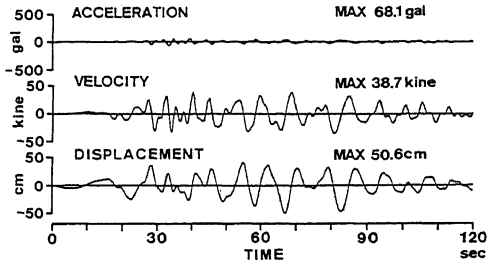

Fig. 5 Calculated earthquake motion (SW-NE) at Hongo in Tokyo

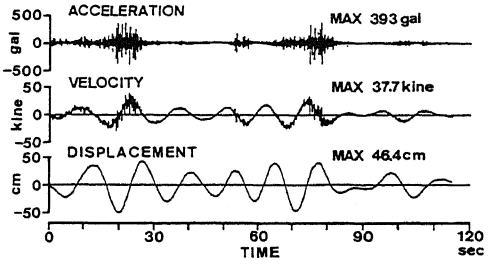

Fig. 6 Actual earthquake motion(SW-NE) observed at Hongo in Tokyo during the Great Kanto earthquake of 1923

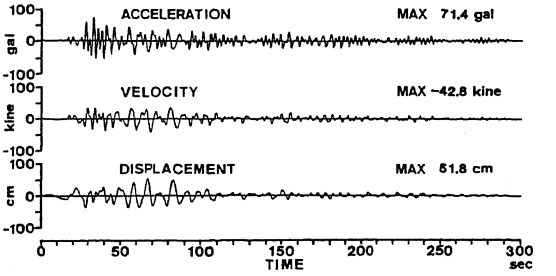

Fig. 7 Calculated earthquake motion (N123°E) in Tokyo

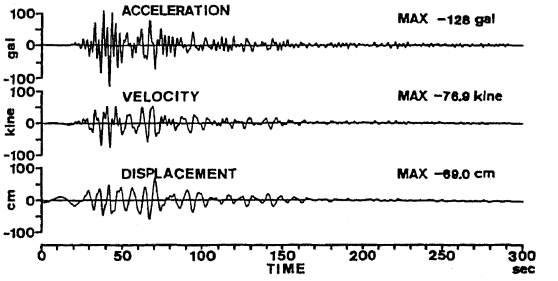

Fig. 8 Calculated earthquake motion (N128°W) at site P

Combining the NS and EW components, the earthquake motion in the azimuth (N123°E) where maximum displacement occurred is calculated. The earthquake motion (N123°E) is shown in Fig. 7. The amplitude of acceleration is not a negligible value in part of coda after the strong earthquake motion. As pointed out by Morioka(Ref. 6), such a ground motion agrees well with the record of the Imamura type seismograph and Dr. Imamura's own experience. From the analyses of locus of ground motion and evolutionary power spectrum(Ref. 7) of the acceleration wave, it can be point out that the surface waves are predominant in the major part of the calculated motion. The Rayleigh wave is predominant at about 40 sec after the rupture of the fault, and the Love wave is predominant at about 70 sec.

Earthquake motion at site P in Chiba prefecture Fig. 8 shows the earthquake motion at site P in the azimuth (N128°E) where maximum displacement occurred. Site P is located at the edge of the fault plane as shown in Fig. 1. From the analyses of elemental waves from each point source and evolutionary power spectrum(Ref. 7), it can be found that the motion at site P is affected strongly by elemental waves excited from near the observation site, and component of the body waves are predominant.

Velocity response spectra Fig. 9 shows the velocity response spectra Sv of the earthquake motions with the damping ratio h=0.5% in Tokyo and at site P. In the calculation, the earthquake motions shown in Figs. 7 and 8 are used. Maximum value of Sv is about 380 kine in Tokyo and about 590 kine at site P, which correspond to the periods of 8.5 and 6.9 sec, respectively. Two peak values of Sv in Tokyo are at periods of about 4-5 and 8-9 sec. These periods correspond to the predominant periods of the Rayleigh and Love waves, respectively. But in the actual earthquake motion (SW-NE component in Fig. 5), there is one peak value of Sv at about 13 sec. This difference in Sv values is thought to stem from the characteristics of Ewing-type seismograph and assumption of the homogeneous layered medium in the calculation. Five peak values of Sv at site P correspond to predominant periods of surface waves and SH waves excited from point sources far from and near observation site, respectively.

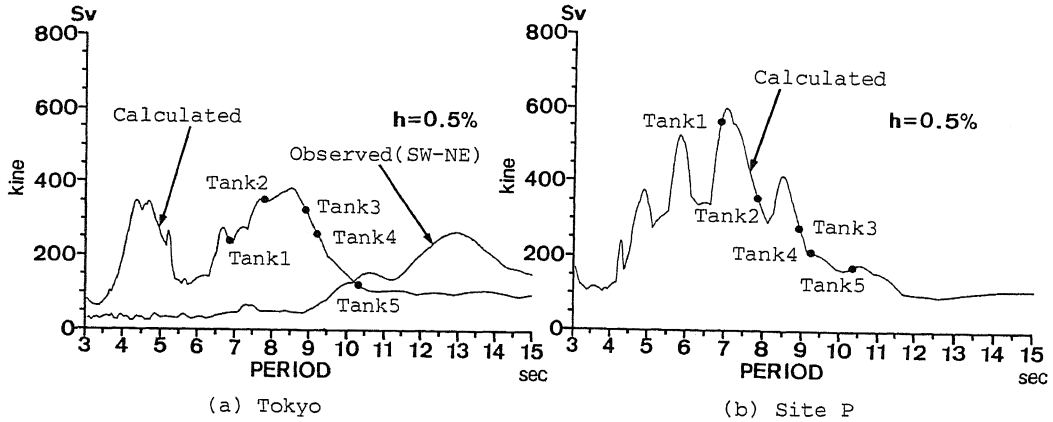

(a) Tokyo (b) Site P

Fig. 9 Velocity response spectra Sv (damping ratio h=0.5%)

SLOSHING WAVE RESPONSE IN LARGE TANKS

The response of sloshing is calculated by the axisymmetric linear potential theory. In the calculation, modes of from the 1-st through the 10-th modes are included. The damping ratio is assumed to be 0.5%. Five kinds of tanks with capacities ranging from 40,000kl to 100,000kl are analyzed. Table 3 shows the diameter of tank, the depth of liquid and the natural periods of sloshing. The earthquake motions shown in Figs. 7 and 8 are used in the response analysis.

Maximum sloshing wave heights are shown in Table 4. The occurrence time of maximum wave height is also shown in parenthesis in Table 4. The response of the sloshing wave height at the sidewall of the tank are shown in Figs. 10 and 11. Figs. 10(a) and 11(a) show the response wave heights of the tank 1 in Tokyo and at site P, respectively. The sloshing wave in Tokyo becomes maximum at about 60 sec, decreases with time, and grows again. On the other hand, at site P, sloshing wave grows gradually in the first mode, reaches maximum at about 100 sec, and decreases with time. The causes of this difference are by the following facts. In the first case, predominant period of the ground motion in the time

Table 3 Five kinds of tanks in sloshing calculation

	Diameter D(m)	Depth of Liquid H(m)	Natural period(sec) 1-st	2-nd
Tank 1	42.0	28.9	6.8	4.0
Tank 2	51.5	24.0	7.8	4.4
Tank 3	62.0	21.5	8.9	4.8
Tank 4	62.0	18.3	9.2	4.8
Tank 5	76.0	22.0	10.3	5.4

Table 4 Maximum sloshing wave heights

	Tokyo	Site P
Tank 1	4.1 (63)	9.4 (99)
Tank 2	6.0 (107)	6.6 (74)
Tank 3	6.2 (91)	5.3 (119)
Tank 4	4.7 (79)	3.5 (120)
Tank 5	2.3 (70)	3.4 (102)

m (sec)

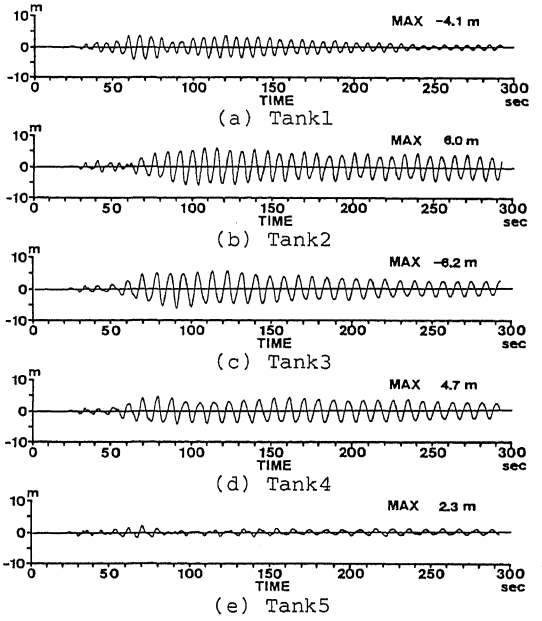

Fig. 10 Response of sloshing wave height at sidewall(Tokyo)

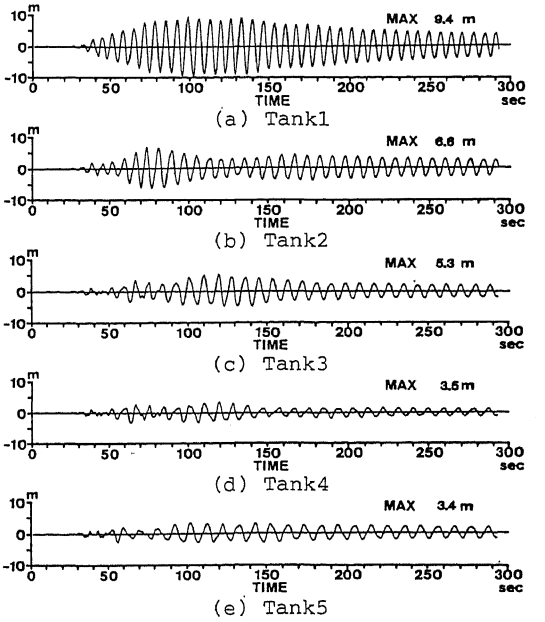

Fig. 11 Response of sloshing wave height at sidewall(Site P)

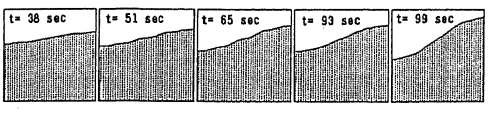

(a) Tank1

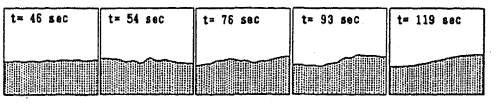

(b) Tank3

Fig. 12 Wave configurations

interval of 70 to 100 sec is different from the natural period of the tank, so that the ground motion keeps down the growth of the sloshing wave. In the second case, the ground motion includes a predominant wave component of period which is almost equal to the first natural period. The growth process of the sloshing wave height for the various tanks at the same site is shown in Figs. 11 (a) and (c). In storage Tank 1, the sloshing wave grows gradually in the first mode from the beginning. On the other hand, in storage tank 3, the sloshing wave grows in the second and third modes as well as the first mode, and after reaching maximum wave height, the wave oscillates in the first mode.

Fig. 12 shows the growth of wave configurations of tanks 1 and 3. In tank 1, the sloshing wave grows in the first mode. In tank 3, the second mode predominates at t=76 and t=93 sec. At t=93 sec, maximum wave height occurs near the center and not at sidewall. This corresponds to large Sv value at the second natural period(4.8 sec) shown in Fig. 9(b).

CONCLUSIONS

Applying the DWFE method to the fault model of the Great Kanto earthquake of 1923 proposed by Matsu'ura, relatively long-period component of a theoretical earthquake motion in the vicinity of the source region is calculated. Then, the sloshing behaviors in large storage tanks are analyzed. Results of this paper are summarized as follows:

1) In Tokyo, maximum displacement and velocity of the calculated earthquake motion agrees well with those of the observed data. From the results of evolutionary power spectrum and velocity response spectra Sv, it is clarified that the surface waves have a large effect on the response of sloshing behavior.
2) The maximum horizontal displacement of earthquake motion at site P (Chiba prefecture) which locates at the edge of the fault plane is about 70cm. It is found that the effect of the body wave excited from the point source near site P is very large. Five peaks exist in the Sv value, and Sv value changes remarkably with the period.
3) Sloshing wave heights of 2.3-6.2m in Tokyo, and 3.4-9.4m at site P (in Chiba prefecture) are predicted for large-scale storage tanks.

REFERENCES

1. Olson,A.H.,Orcutt,J.A.and Frazier,G.A.,"The discrete wavenumber/finite element method for synthetic seismograms",Geophys.J.R.astr.Soc.,Vol.77,421-460(1984).
2. Matsu'ura,M.,Iwasaki,T.,Suzuki,Y. and Sato,R.,"Statical and dynamical study on faulting mechanism of the 1923 Kanto earthquake",J.Phys.Earth,Vol.28,119-143(1980).
3. Shima,E.,Yanagisawa,M.,Kudo,K., Yoshii,T.,Seo,K. and Kurota,K., "On the base rock of Tokyo III. Observations of seismic waves generated from the 4th and 5th Yumenoshima explosions", Bull.Earthq.Res.Inst., Vol.53, 305-318(1978)(in Japanese).
4. Aki,K. and Richards,P.G. "Quantitative Seismology Theory and Method", Vol.II, Chapt.14 The seismic source:Kinematics,799-849,W.H.Freeman and Co.(1980).
5. Day,S.M., "Finite element analysis of seismic scattering problems", Ph.D.Thesis, University of California at San Diego(1977).
6. Morioka,T., "The ground motion of the Great Kwanto earthquake of 1923",Trans. of Architectural Institute of Japan, No.289,79-88(1980).
7. Kameda,H., "On a method of computing evolutionary power spectra of strong motion seismograms", Proc. of Japan Society of Civil Engineers, Vol.235, 55-61(1975)(in Japanese).
8. Sogabe,K. and Shibata,A., "Response analysis on sloshing of liquid in a cylindrical storage I —Basic equation and response to sinusoidal input—", 'Seisan Kenkyu' Monthly Journal of Institute of Industrial Science, University of Tokyo, Vol.26,No.3,119-122(1974)(in Japanese).